Lafia Journal of Scientific & Industrial Research (LJSIR), Vol. 4(1), 2026
p-ISSN: 3026 – 9288 e-ISSN: 3027 – 1800 pages: 176–188
https://lafiascijournals.org.ng/index.php/ljsir/index ⇒ Published by the Faculty of Science,
Federal University of Lafia, Nasarawa State, Nigeria

Geochemical Characterization and Mineralization Potential of Basement Rocks in Arum, North-Central Nigeria

A. S. Usman[1], A. B. Segun[2], A. M. Kaura[1*], A. S. Mukaila[1], Y. Andarawus[1], I. M. Sanusi[1], S. Aliyu[1], L. O. Agho[1] & T. E. Bamidele[3]

[1]Department of Geology, Federal University of Lafia, Nasarawa State, Nigeria
[2]Department of Geology, Nasarawa State University, Keffi, Nigeria
[3]Department of Geology and Mineral Science, Kwara State University, Malete, Nigeria

Abstract

Geochemistry and mineral potential of Arum and environs, North Central Nigeria, was carried out to evaluate and characterize the major and trace elements composition in the rocks and stream sediments of the area. Sixteen rock samples from four lithologies and eighteen stream sediments were collected at strategic locations. The samples were geochemically analyzed for major and trace elements using X-ray fluorescence. The silica concentrations in the pegmatite and granodiorite range from 76.0 to 79.95 weight percentage (wt%) and 74.09 to 76.01 weight percentage (wt%), respectively, according to the analytical results, which showed that both minerals are extremely siliceous. All of the lithologies in the study area exhibit a slightly consistent concentration of Al_2O_3, with the ranges being 13.48 to 15.06 in fine to medium grain granite gneiss, 14.65 to 15.91 in medium grain banded gneiss, 13.26 to 14.3 weight percent (wt%) in granodiorite, and 14.26 to 14.65 weight percent (wt%) in pegmatite. The TAS plot of silica saturation index indicates that Arum rocks are granitic, and the aluminum saturation index indicates that Arun rocks are primarily peraluminous. The geochemical concentration shows the spatial distribution and enrichment. The bar-chart concentration plots revealed an uneven anomalous concentration of thorium (Th), tantalite (Ta), niobium (Nb), tin (Sn), and rubidium (Rb) in ppm, compared to their respective background concentration, which revealed a positive anomalous concentration. Arum shows allochthonous mineralization that is structurally controlled and can be regarded as been mineralized in Th, Nb, Sn, U, and Ta.

Keywords: Arum, geochemistry, mineralization, petrogenesis, x-ray-fluorescence, peraluminous, pathfinder

Article History

Submitted
January 11, 2026

Revised
April 10, 2026

First Published Online
April 18, 2026

Correspondences
A. M. Kaura ✉
am.kaura@science.fulafia.edu.ng,
kaurite80@gmail.com

doi.org/10.62050/ljsir2026.v4n1.727

Introduction

The search for viable economic deposits, particularly in Nigeria, has gained renewed attention due to the rise in demand for trace elements such as tantalum (Ta), niobium (Nb), tin (Sn), cerium (Ce), thorium (Th), and silver (Ag) worldwide. The primary exploration target in Nigeria is the North-Central region [1]. The study area (Arum) is flooded by miners due to increase in demand for rare elements such as gold (Au), tin (Sn), tantalum (Ta), niobium (Nb), beryl (Be), monazites, and zircon (Zr) for industrialization and economic expansion. Aluminum (Al), copper (Cu), silver (Ag), lead (Pb), lithium (Li), manganese (Mn), nickel (Ni), zinc (Zn), and other minerals like indium (In), molybdenum (Mo), and neodymium (Nd) are among the metals and minerals that are anticipated to have increased demand (https://www.worldbank.org). However, research has been conducted in the north central region of Nigeria for various targets related to the mineralization potential of different rocks and REEs, including [2–4], and others. [5, 6] undertook a reconnaissance work at Wamba and Jema'a on the metallogenetic features of the basement and highlighted the economic viability of central Nigeria (Wamba in particular). In the work of [7] he concluded that, the gabbroic intrusion of the Sha-kaleri Younger Granite Complex is alkaline in nature, while the Arum rocks within the same complex are ratherCal alkaline composition, this geochemical variance may be due to the effect of metasomatism and/or alteration on rocks around Arum.

The Basement Complex rocks in the study area have received little attention regarding the geochemistry of various rock types, as evidenced in the literature. It has only dealt with the economic parameters of the rare metal contents within the pegmatites. Little is known about the adjoining parent granites and other rock types and their economic potentials apart from the pegmatite studies. Also, due to little attention given to the

geochemistry and mineral potential of other rocks in Arum, this work was therefore necessitated by the need to unravel the mineral potential of Arum, through a geochemical study of the rocks, soil and stream sediments using the major and trace elements composition as widely used to discover mineral signatures of economically valuable deposits.

The content, distribution, and behavior of the chemical elements (both major and trace) in soil depend on many factors mainly related to the mineralogical and geochemical features of the bedrock [8, 9]. They are influenced by the development and intensity of weathering and soil formation processes (physical, chemical, and biological). Additionally, they can sometimes be affected by minor phenomena such as anthropogenic pollution [10], as well as the ratio and chemical composition of atmospheric depositions [11].

Materials and Methods

The work was guided through the application of base map, extracted from topographical map. The base map was gridded along regular interval of space using sufer software with all the locations of samples (rocks, soil and sediments) inputted as shown in Fig 2. Satellite imagery map of the area of research was developed with ArcGIS to have a 2D view of the region's topography Fig 1. Rocks, soil, and stream sediments samples were collected. Sixteen unweathered rocks samples were collected from four different lithologies. The representatives' samples were kept in envelope and labeled. Eighteen stream sediments were carefully collected at an average depth of 30 cm and stored in envelopes, the sample were dried at room temperature. Rock samples were divided, with a portion going for thin section analysis for petrography studies as the other portion is prepared for geochemical analysis. Rock thin section was prepared for study using petrographic microscope at the petrographic laboratory of Nasarawa state university, Keffi. X-rays Fluorescence analysis was employed for compositional geochemical studies of rocks and soils, which was carried out at the Center for Solid Mineral Research and Development (CSMRD) Kaduna. Result was subjected to different statistical analysis with appropriate computer software (Rock plots, Excel, Sufer, ArcGIS and GCDkit) were used for data evaluation as discussed in subsequent chapters of this research. The research flow chat is used for illustration of how the research was carried out (Fig 3).

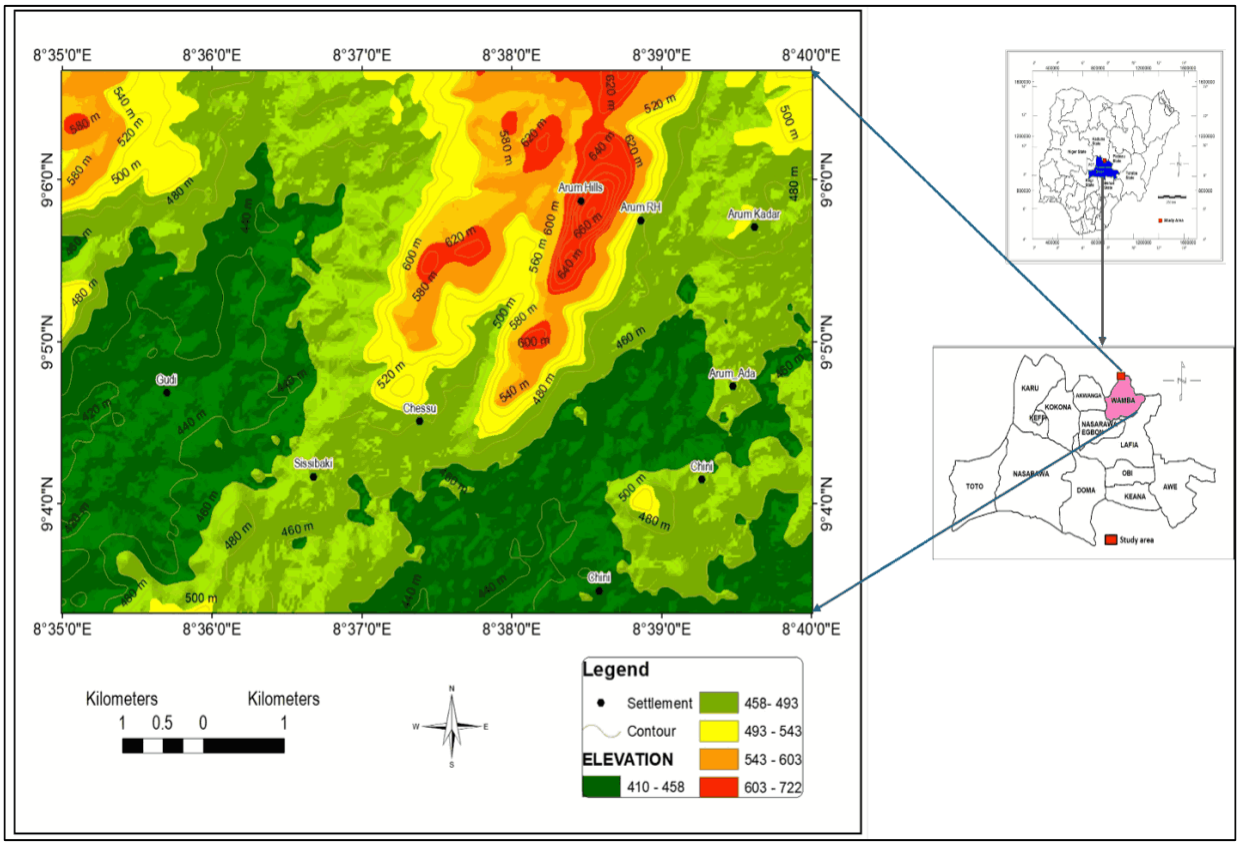

Figure 1: Satellite image showing the topography of Arum and environs

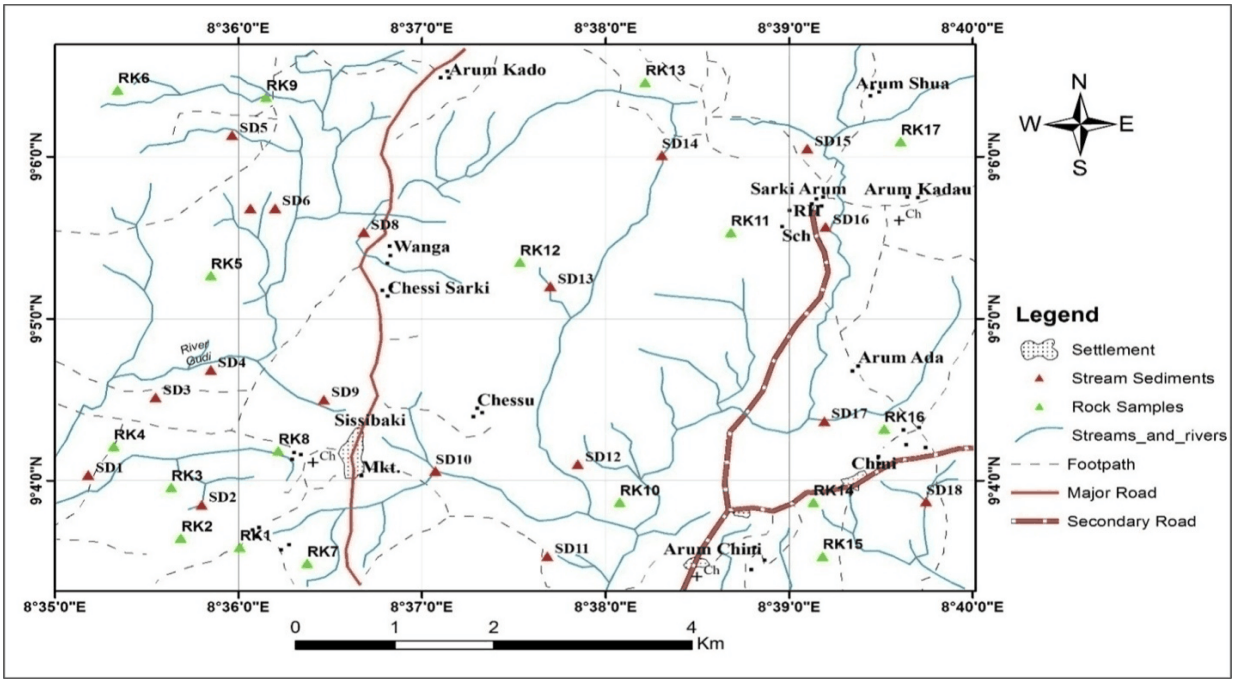

Figure 2: Location map of the study area showing sampling points for rocks and stream sediments, drainage network, and accessibility routes

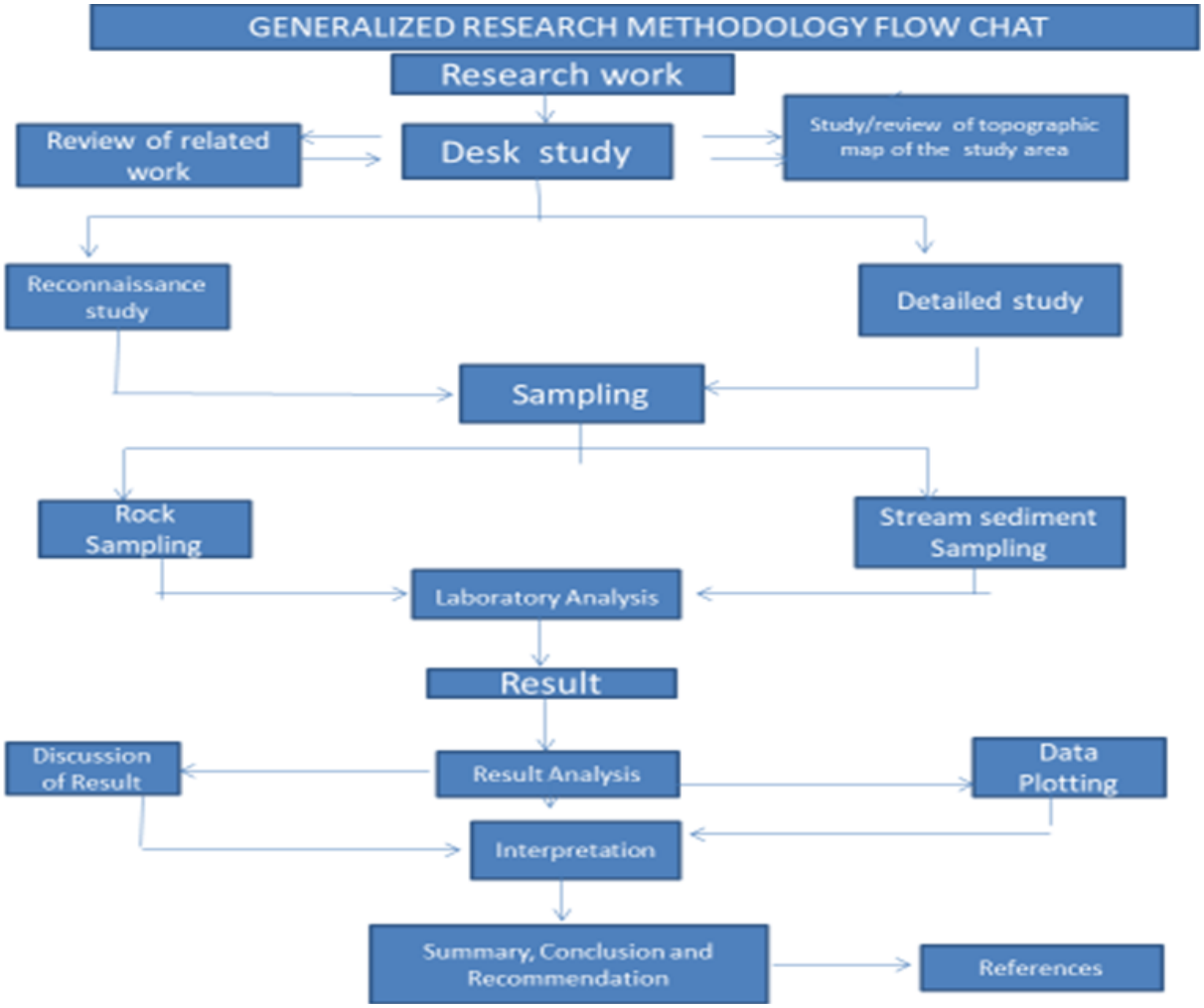

Figure 3: An illustration of the research flowchart

Results and Discussion

Geological settings

The study forms part of Kura sheet 189SW, lies within longitude $8^0 35' 00''$E to $8^0 40' 00''$E, latitude $9^0 03' 20''$N to $9^0 06' 40''$N (Fig. 1) and a total area of 50 km^2. The area is bordered by the Sha-kaleri Younger Granite Complex to the North. Also, the area covers the towns of Arum Sarki, Arum Shua, Arum Kado, Wanga, Sisimbaki, Chessu, Chessu Sarki and part of Marmara in Wamba, North Central Nigeria. The area is characterized by the highland of the Arum hills, which cover part of Chessu and Arum Shuwa, with other adjoining small hills. Based almost exclusively on Rb-Sr dating, is that the Nigerian Basement evolved during a long and polyphase tectono-metamorphic history, including Liberian (2700±200 Ma), Eburnean (2000±200 Ma), Kibaran (1100±200 Ma), and Pan-African (600±150 Ma) events [12–15]. Arum is situated within the Nigerian Pan-African Basement, part of the Upper Proterozoic-Lower Phanerozoic mobile belt situated between the West African Craton to the West and Congo Cratons in the South East [16]. The belt is interpreted to have evolved by plate tectonic processes which involved continental collision between two blocks, the passive continental margin of the West African Craton and the active continental margin (Pharusian belt) of the Tuareg Shield about 600 Ma [17–21]. The Nigerian Basement Complex lies in the reactivated part of the belt [13].

The research revealed three (3) dominant differentiated lithologic units, namely, (1) granodiorite occupied 23 %, (2) medium-grained banded gneiss 40 %, and (3) fine to medium-grained granite gneiss 33 %, which were intruded by Pegmatite occupying 4 % (Fig. 4). The pegmatite veins displayed a NE-SW, NE-SW and NNW-SSW trends, which align with the structures imposed during the later stage of Pan-African tectonic activities [22], with slight variation in grain sizes and colours, presumably due to, to varying degrees of metamorphism or mineral remobilization. The pegmatite occurred sparingly within the study area, though it formed a small ridge at longitude $08^{\circ}38'11.01''$ and latitude $09^{\circ}03'32''$ located approximately 700 meters northeast of Arum Chini.

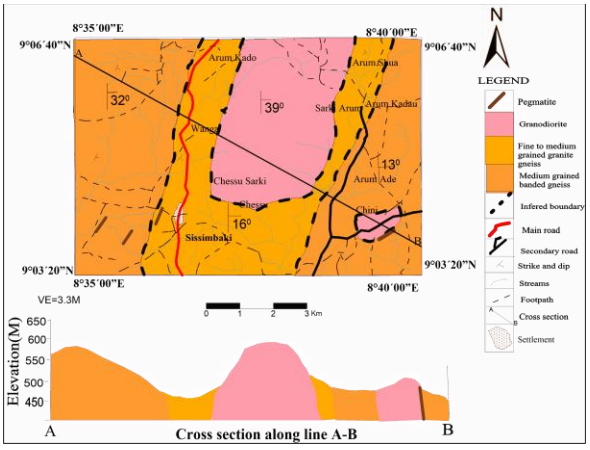

Figure 4: Geological map of Arum and environs depicting major lithological units

Petrology

Field observation shows that the granodiorite, medium-grained banded gneiss, fine to medium-grained granite gneiss and pegmatite were petrographically analyzed. Granodiorite shows the presence of quartz, plagioclase, orthoclase, and muscovite. Medium-grained banded gneiss showed the presence of quartz, plagioclase, biotie and accessory mineral (microcline). Fine to medium-grained granite gneiss displayed quartz, plagioclase, and biotite. Pegmatite shows the presence of quartz, plagioclase, orthoclase, and muscovite.

Whole rock geochemistry

This chapter presents the statistically analyzed geochemical data of the major and trace elements obtained from the geochemically analyzed rocks, soil and stream sediments samples collected from the study area. A total of thirty-four (34) samples (16 rocks and 18 stream sediments) were analyzed for major and trace elements, including rare earth elements (REE). These samples include representative samples of the granodiorite, fine to medium-grained granite gneiss, medium-grained banded gneiss, pegmatite and the stream sediments. The elements were analyzed using an X-ray fluorescence spectrophotometer.

The whole rock geochemical result, as shown in Table 1, is the data of major elements oxides of the whole rock samples in percentage (%) composition. Table 2 is a presentation of statistically treated geochemical data of the major oxides in percentage (%) composition. Table 3 shows the trace elements data obtained from whole rock analysis of a sample collected in parts per million (ppm). Table 4 is a data of trace element concentrations in stream sediments around Arum in parts per million (ppm). Table 5 is a range of trace elements compositional in whole rock samples in parts per million (ppm). The whole rock geochemical data of Table 2 is used for the plotting and classification of rocks as shown in Figs 5, 6, 7 and 8. The Table 4 data was used for different geochemical plots and diagrams to characterize the rocks and their geochemical association. The major elements geochemical data were used for rock classification, while the trace elements data were adopted to identify the zone of anomalous concentration. Results of the geochemical analyses of the representative samples from four different lithologies vary across all the lithologies, reflecting their mineralogical and lithological differences.

The importance of making available geochemical concentrations of major and trace elements of bedrock outcropping in the vicinity of Arum and its environs lies in the possibility of obtaining real correlation structures where soils are compared directly with the mean compositions of their parent rocks. This comparison leads to evaluating the contribution of different rock types on the chemical composition of each soil sample and to identifying anomalies of some elements [23]. The data reveal high and moderate enrichments in SiO_2 and Al_2O_3, respectively, in all the rock types, resulting from their high contents in quartz and aluminosilicate minerals. These high siliceous and

peraluminous compositions provide the type of silicic and acidic environments necessary for tourmaline and beryl crystallization [22].

Table 1: Major elements oxides data of the whole rock samples of the study area (wt%)

S/N	Sample Type	SiO_2	AI_2O_3	Fe_2O_3	Na_2O	K_2O	CaO	MgO	TiO_2	MnO	P_2O_5	LOI	Total
1	RK1	68.5	14.3	4.98	0.53	0.98	4.51	3.47	2.01	0.32	0.04	0.33	99.97
2	RK2	71.57	13.48	1.08	2.38	4.98	5.49	0.64	0.94	0.04	0.06	0.49	100.95
3	RK3	72.93	16.26	1.21	2.11	6.01	1.02	0.92	0.31	0.04	0.01	0.18	101.36
4	RK4	73.14	16.65	1.74	2.14	4.03	0.15	0.56	1.02	0.14	0.01	0.42	100.04
5	RK5	76.09	14.13	0.93	2.09	5.07	0.44	0.43	0.01	0.11	0.06	0.74	99.940
6	RK6	69.21	15.91	5.62	5.35	2.55	2.37	0.54	0.78	0.07	0.02	1.13	101.00
7	RK7	74.09	14.07	1.04	2.41	5.06	1.91	0.73	0.5	0.06	0.03	0.10	100.00
8	RK8	68.34	15.02	4.66	0.49	0.77	4.72	3.62	1.86	0.12	0.03	0.37	100.00
9	RK9	74.13	14.38	3.89	2.41	1.24	2.41	0.41	0.7	0.13	0.02	0.28	100.42
10	RK10	72.92	14.26	0.85	2.2	5.61	2.09	2.49	0.04	0.14	0.10	0.82	99.90
11	RK11	73.02	15.06	3.85	2.38	1.24	2.35	0.41	0.65	0.16	0.03	1.85	99.15
12	RK12	66.24	14.81	5.46	2.55	1.79	5.04	1.61	1.85	0.30	0.35	1.35	100.65
13	RK13	76.82	14.47	0.79	2.38	4.3	0.14	0.55	0.03	0.16	0.20	0.35	99.80
14	RK14	64.82	15.69	6.56	2.62	1.81	5.04	1.65	1.85	0.31	0.80	1.23	99.20
15	RK15	75.76	13.74	1.03	2.17	4.65	1.85	0.16	0.46	0.03	0.05	1.10	101.00
16	RK16	76.95	14.35	1.01	2.21	3.98	0.12	0.58	0.03	0.17	0.01	0.59	100.00

Table 2: Major and trace elements ratio of the whole rock samples of the study area

S/N	Sample	K	Na	K/Rb	K_2O/NaO	Na_2O /Al_2O_3	K20 /Al_2O_3	Na_2O /K_2O	Na_20 +K_2O	Na_2O+ K_2O- CaO	Al_2O_3/CaO+ Na_2O+K_2O	Al_2O_3/ Na_2O+K_2O	Zr/$Ti0_2$	y+Nb
1	RK1	0.814	0.4302	0.0075	1.690	0.041	0.069	0.592	1.56	-2.95	2.356	9.167	56.2	10
2	RK2	4.134	1.766	0.0225	2.092	0.177	0.369	0.478	7.36	1.87	1.049	1.832	117.0	45
3	RK3	4.159	1.565	0.0293	2.374	0.159	0.378	0.421	7.12	6.1	1.629	1.862	331.3	27
4	RK5	3.346	1.588	0.0166	1.883	0.146	0.275	0.531	6.17	6.02	2.318	2.374	5550.0	71
5	RK12	4.209	1.55	0.0417	2.426	0.148	0.359	0.412	7.16	6.72	1.859	1.973	10.4	7
6	RK18	2.217	3.969	0.0070	0.477	0.336	0.160	2.098	7.9	5.53	1.549	2.014	138.5	13
7	RK30	4.201	1.787	0.0143	2.100	0.171	0.360	0.476	7.47	5.56	1.500	1.884	226.0	15
8	RK6	0.639	0.364	0.0021	1.571	0.033	0.051	0.636	1.26	-3.46	2.512	11.921	63.4	39
9	RK4	1.029	1.788	0.0036	0.515	0.168	0.086	1.944	3.65	1.24	2.373	3.940	147.1	22.4
10	RK17	4.657	1.632	0.0235	2.550	0.154	0.393	0.392	7.81	6.72	1.602	1.826	3025.0	28.5
11	RK16	0.199	1.766	0.0008	0.101	0.158	0.082	1.919	2.62	0.27	3.030	4.160	156.9	41
12	RK22	1.486	1.892	0.0057	0.702	0.172	0.121	1.425	4.34	-0.61	1.579	3.412	106.5	10
13	RK10	3.569	1.766	0.0142	1.807	0.164	0.297	0.553	6.68	6.54	2.122	2.166	4233.3	72
14	RK13	1.503	1.944	0.0062	0.691	0.167	0.115	1.448	4.43	-0.61	1.165	3.542	68.1	33
15	RK28	3.86	1.609	0.0117	2.143	0.158	0.338	0.467	6.82	-4.97	1.585	2.015	258.7	38
16	RK34	3.304	1.639	0.0089	1.801	0.154	0.277	0.555	6.19	6.07	2.274	2.318	7166.7	68

Table 3: Trace element data of whole rock samples of the study area (ppm)

S/N	Sample ID	Rb	Sr	Cr	Th	U	V	Ta	Nb	Co	Cu	Sn	Ag	Au	Ba	Zr	As	Pb	Ni	Zn	Ga	Y
1	RK1	109	236	97	8	11	7	126	12	09	13	18	12	-	212	113	5	-	07	06	12	4
2	RK2	184	437	75	5	7	19	118	18	2	19	28	11	-	307	110	4	2	08	09	16	27
3	RK3	142	392	82	13	9	26	84	16	1	34	102	09	-	733	106	6	1	08	11	4	11
4	RK4	201	311	68	14	6	51	152	46	25	41	271	35	-	606	111	4	1	11	35	21	25
5	RK5	101	279	72	9	12	16	323	4	1	35	89	15	-	471	104	7	1	12	15	4	3
6	RK6	302	402	49	5	8	13	103	12	06	4	09	21	-	550	108	8	3	13	11	1	1
7	RK7	293	398	59	3	9	15	104	8	04	34	11	17	-	486	113	9	9	10	12	12	7
8	RK8	311	374	72	2	9	23	103	7	-	39	8	18	-	867	118	6	18	13	06	11	32
9	RK9	287	413	82	4	7	18	116	21	2	13	08	21	-	716	103	8	13	07	08	2	14
10	RK10	198	382	94	5	9	16	117	18	08	11	08	23	-	127	121	6	13	05	09	0.6	1..5
11	RK11	212	407	74	4	8	11	105	23	1	42	10	21	-	512	102	9	7	05	09	2.4	18
12	RK12	261	426	78	13	9	61	39	3	2	24	08	16	-	649	197	9	11	07	07	9	7
13	RK13	252	502	73	19	12	94	336	48	24	21	131	36	-	784	127	7	3	06	34	1	24
14	RK14	241	511	67	7	5	14	66	12	2	13	11	22	-	727	126	7	6	08	10	2	21
15	RK15	330	491	81	4	6	24	109	63	0.5	8	93	21	-	365	119	8	11	08	19	7	32
16	RK16	370	501	77	17	15	81	343	57	3	28	171	38	-	812	215	9	17	07	32	14	41

Table 4: Trace elements concentration in stream sediments of the study area (ppm)

Sample ID	Rb	Sr	Cr	Th	U	V	Ta	Nb	Co	Pb	Cu	Sn	Ag	Au	Ba	Zr	As	Ni	Zn	Ga	Y
SD1	149	255	118	89	8	17	152	161	0.6	62	28	34	38	-	175	327	22	51	213	9	13
SD2	161	278	111	87	7	11	173	175	0.5	49	32	61	31	-	131	279	21	72	239	2	10
SD3	161	352	128	79	8	21	154	182	0.5	40	27	43	24	-	124	87	7	42	311	11	4
SD4	204	182	218	68	12	18	179	172	0.2	82	41	48	21	-	189	249	13	74	328	21	31
SD5	131	282	213	89	15	19	153	193	1.5	44	48	71	28	-	194	320	9	81	136	4	24
SD6	145	255	210	79	9	10	172	174	1.2	21	52	22	31	-	184	187	13	79	155	31	9
SD7	178	195	217	89	8	4	181	164	1.5	9	52	31	28	-	201	191	11	72	212	11	3
SD8	127	189	214	81	14	20	171	172	2	5	49	40	31	-	131	311	7	75	309	42	32
SD9	216	272	159	67	8	27	197	191	0.5	13	52	51	14	-	250	71	22	64	355	6	16
SD10	184	145	141	63	7	12	174	175	0.8	71	34	50	23	-	141	189	13	67	247		9
SD11	172	252	136	65	8	18	153	191	1.1	4	47	42	28	-	109	67	16	83	322	9	5
SD12	158	240	217	74	7	14	194	162	3.1	18	45	40	27	-	178	121	24	94	336	1	13
SD13	141	212	221	95	8	27	181	172	0.3	3	31	17	28	-	155	321	15	54	324	12	27
SD14	210	180	118	78	11	13	157	151	3.4	7	26	62	28	-	157	77	23	79	536	22	19
SD15	192	214	213	73	12	17	172	171	0.2	21	69	41	27	-	158	109	21	52	835	12	36
SD16	213	261	11	74	0	19	147	162	1.6	28	36	23	26		210	261	16	46	948	17	40
SD17	310	251	121	92	11	20	164	61	2.3	5.6	41	24	21		310	271	21	72	184	21	71
SD18	291	240	108	72	31	46	181	179	4.1	7.2	52	36	25	-	311	256	24	81	174	31	81

Table 5: Range of trace elements in the whole rock sample (ppm)

Elements	Whole rock fine to medium-grained granite gneiss (FMGGG)	Whole rock medium-grain banded Gneiss (MGBG)	Whole rock granodiorite G	Pegmatite P
Ta	104 – 117	39 – 103	84 – 109	152–343
Nb	8 – 23	3 – 12	16 – 63	46–57
Th	4 – 8	2 – 13	5 – 81	9–19
U	7 – 9	5 – 9	6 – 11	6 – 15
V	11 – 16	13 – 61	13 – 26	9 – 15
Rb	198 – 293	241 – 370	142 – 330	201–370
Sr	311 – 398	374 – 511	392 – 491	279 – 511
Sn	8 – 11	08 – 11	89 – 102	131 – 271
Ag	16 – 22	16 – 22	9 – 21	35 – 38
Zr	113 – 107	113 – 197	104 – 119	111–215
As	6 – 9	6 – 9	6 – 9	4 – 9

Table 5 above shows the range of concentration of trace elements in different lithologic units across Arum. The Table shows the varied concentration of elements in different rock units of the Arum. As presented in Table 5, pegmatite has a high concentration of Ta, followed by fine to medium-grained granite gneiss and granodiorite, while medium-grained banded gneiss has the least concentration of Ta. Rb and Sr occurred significantly in all four rock types. This significant concentration across all the rocks may be attributed to the incompatible nature of Rb and Sr. Sn concentration in pegmatite is very high, followed by granodiorite, compared to fine to medium grain granite gneiss, and medium grain banded gneiss has the least concentration in equal proportion. Th, U, V, and As have very low concentrations across all the rocks; this may be a result of their high compatibility and solubility in aqueous or magmatic fluids. Table 4 of the stream sediments data is used in producing geochemical concentration zones overlain by the geology of the Arum and environs, as it is shown in Figs 9, 11, 13, 15 and 17 are used in determining areas of anomalous concentration in the study area. While Figs 10, 12, 14, 16 and 18 are bar chats of platted geochemical data of Table 4 against their respective background values.

Geochemical interpretation

The geochemistry and mineral potential of Arum is a characterized sum total chemistry of the varying rock units and surrounding sediments. Data gotten from the geochemical analyses of rocks and stream sediments were normalized to percentage (%) units for the major oxides, while the trace elements were used in parts per million (ppm) units.

Silica saturation

The major element geochemistry of the rocks shows that the rocks are highly siliceous ranging between 68.50–74.13 % in fine to medium grained granite gneiss, 68.34–77.14 % in medium grained banded gneiss, 74.09–76.09 % in granodiorite and 76.01–76.95 % in pegmatite, with pegmatite and granodiorite haven the highest percentage of silica (acidic composition), this is revealed in silica saturation index of TAS Na_2O+K_2O vs SiO_2 [24]. Fig. 5 shows that predominantly, all the rocks fall within the portion of

granite and granodiorite, indicating the acidic nature of the study area. On the composition of iron (Fe) in the rocks, the gneisses have a greater percentage, ranging from 0.85–4.98 % in medium-grained granite gneiss RK8 and 0.75 – 5.62 % in medium-grained banded gneiss RK6.

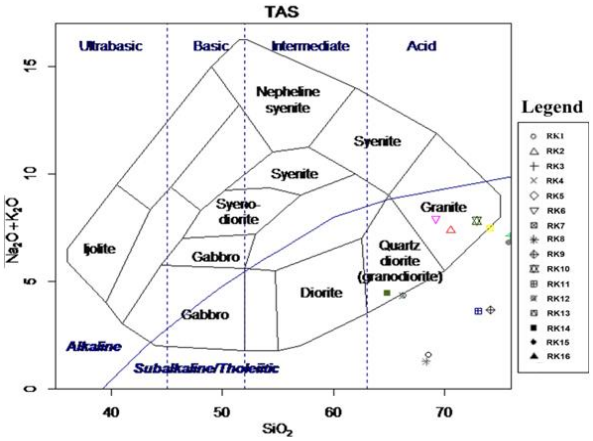

Figure 5: TAS diagram [24] illustrating rock classification based on silica content, indicating granitic to granodioritic composition of Arum rocks

Alkali composition

Figure 6, AFM plot [25] shows the Alkali-lime index and depicts the total sum composition of alkali Na_2O, K_2O and CaO higher than the Fe_2O_3, (5.35 + 5.69 + 5.49 = 16.53 > 15.91 %) classifying the rocks under the calc-alkaline group members.

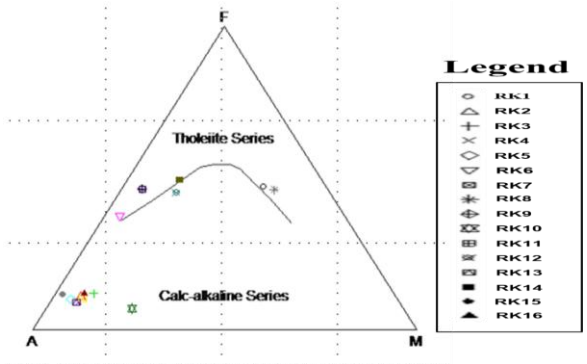

Figure 6: AFM diagram [25] showing alkali-lime index and classification of Arum rocks as calc-alkaline

Alumina saturation

Statistically, analyzed geochemical data in Table 1: A/CNK > 1 and A/NK > 1, where A = Al_2O_3, CNK= CaO + Na_2O + K_2O and NK = Na_2O + K_2O), indicates that 90 % of the investigated rocks are peraluminous in nature, they have high aluminum content in relation to alkali metal, with exception of rocks of the medium-grained banded gneiss that shows metaluminous composition as shown in Fig. 6. The plots of Al_2O_3 vs CaO vs Fe_2O_3 showed that the rocks in the study area are aluminium-rich compared to Fe content (Fig. 7). The alumina saturation index is deduced by the molecular ratio of Al_2O_3 against alkali oxides, which classifies the Arum rocks as peraluminous (A/CNK > 1). Molar plot of Na_2O–Al_2O_3–K_2O as shown in. Fig 7. The ACF plot shows that the rocks are dominantly peraluminous (Fig. 8).

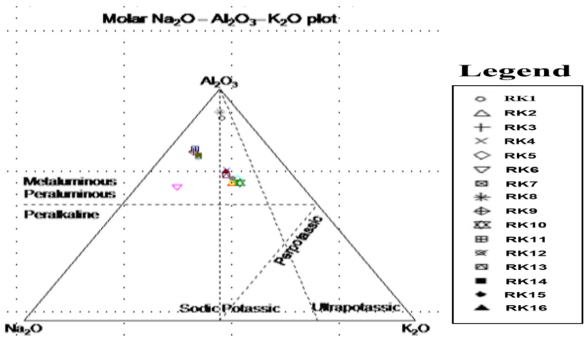

Figure 7: Molar plot showing the peraluminous nature of the rocks of Arum

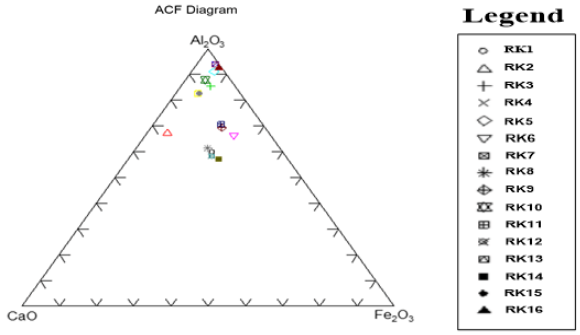

Figure 8: ACF diagram showing relative proportions of Al_2O_3, CaO, and Fe_2O_3, highlighting the aluminum-rich nature of Arum lithologies

Distribution and concentration of elements in soil

Trace elements results from Table 3 were used to plot geochemical concentration map of Niobium (Nb), Tantalum (Ta), Tin (Sn), Thorium (Th) and Uranium (U) (ppm) to determine their distribution pattern and anomalous concentration. Though their concentration varies in some location indicating variation is secondary mineralization probably due to their differences in dissolution and mobility. All the aforementioned elements showed elevated concentration in samples collected around granodiorite, pegmatite and their nearby streams. Fig. 9 shows geochemical concentration map of Niobium (Nb) overlain the geological map, Fig. 10 is a bar chat plot of concentration against crustal abundance, and Fig. 11 is a geochemical concentration map of Tantalum (Ta) overlain the geological map with its bar chat plot (Fig. 12), showing the concentration against its crustal abundance, all shows similar pattern of concentration as

shown, both elements indicates elevated anomalous concentrated around fine to medium grain banded gneiss which share boundary with granodiorite, which could imply both rocks contributes to their concentration. The ranges of trace element concentrations in fine to medium grain granite gneiss, granodiorite and pegmatites, as shown in Table 5 (104-117, 84-109, 152-343 ppm), were found to be the primary sources of the Nb, Ta and Sn that got enriched in the surrounding sediments (secondary enrichment/mineralization). The geochemical concentration map of Tin (Sn) as shown in Fig. 13 and the bar chat in Fig. 14, indicates areas with anomalous concentration. The concentration of Tin (Sn) across the rock types (fine to medium grain granite gneiss 8-11 ppm, medium grain banded gneiss 8-11 ppm, granodiorite 8-11 ppm and pegmatites 131-271 ppm), shows a structurally controlled style of deposition, hence, their concentration in the along-stream channels, sediment and soils. Jatau *et al.* [26] characterized the rocks within Raga Wamba, Central Nigeria and elucidated that the mineralization trend and potential are not only for gold mineralization but for important minerals that may be of high commercial value.

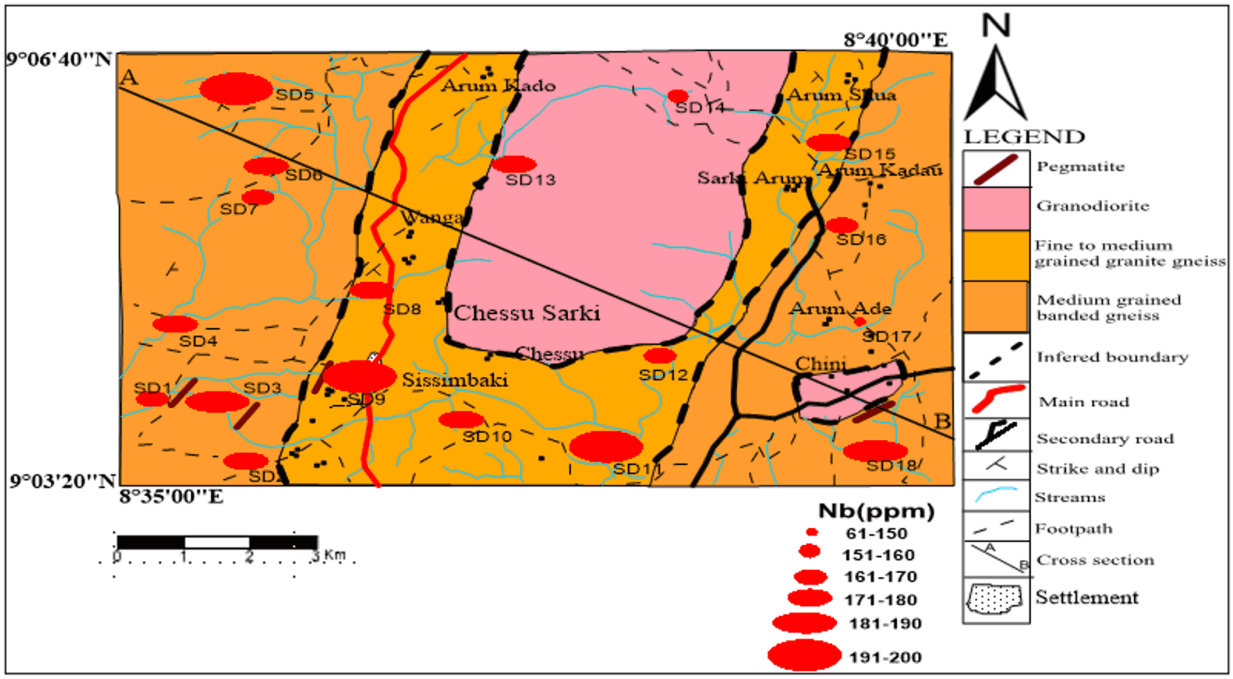

Figure 9: Spatial distribution map of niobium (Nb) concentrations in stream sediments overlain on the geological map of Arum and environs

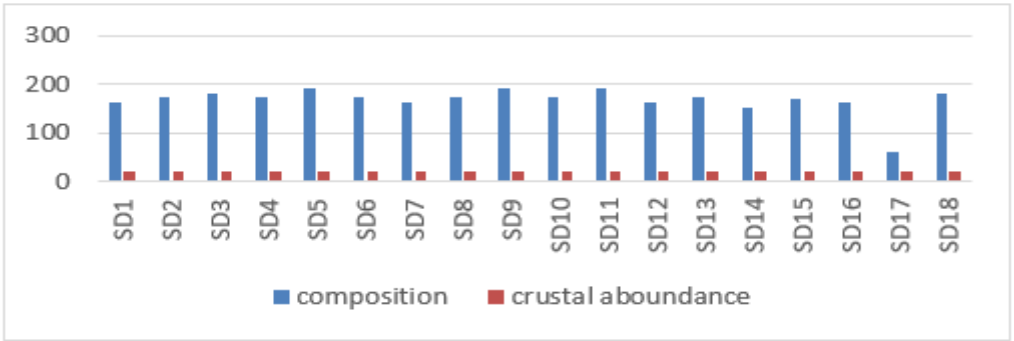

Figure 10: Bar chart illustrating the varying concentration of (Nb) in stream sediment with its crustal abundance

Tantalum (Ta): Tantalum shows high concentration along Sisimbaki and Arum Chini

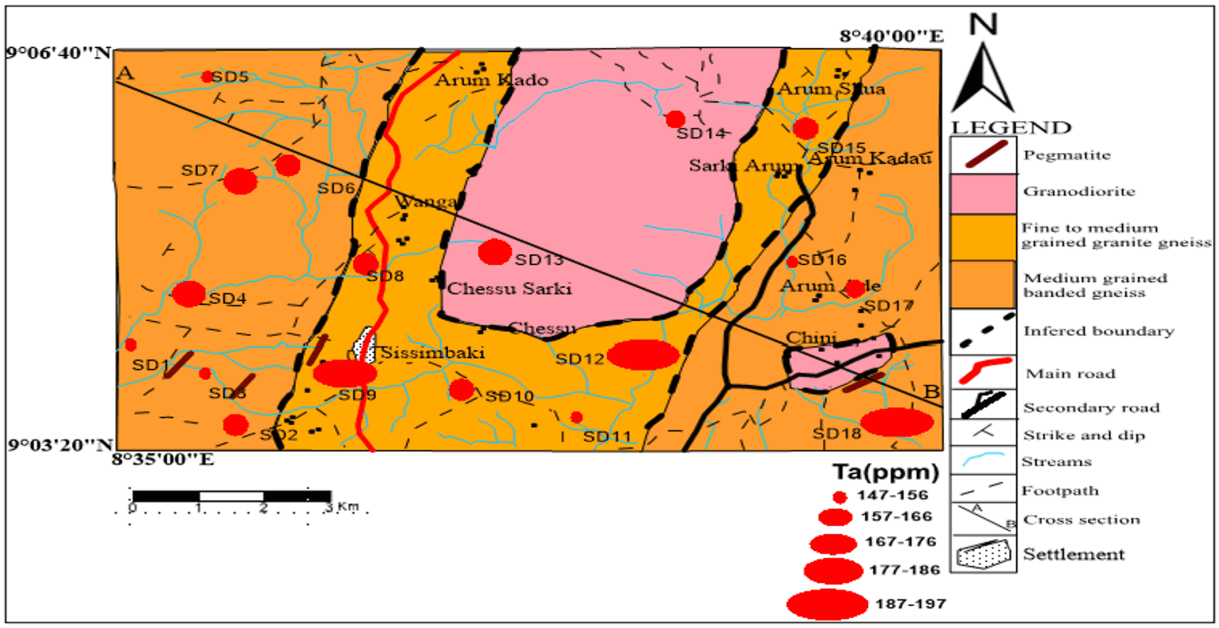

Figure 11: Spatial distribution map of tantalum (Ta) concentrations in stream sediments overlain on the geological map of Arum and environs

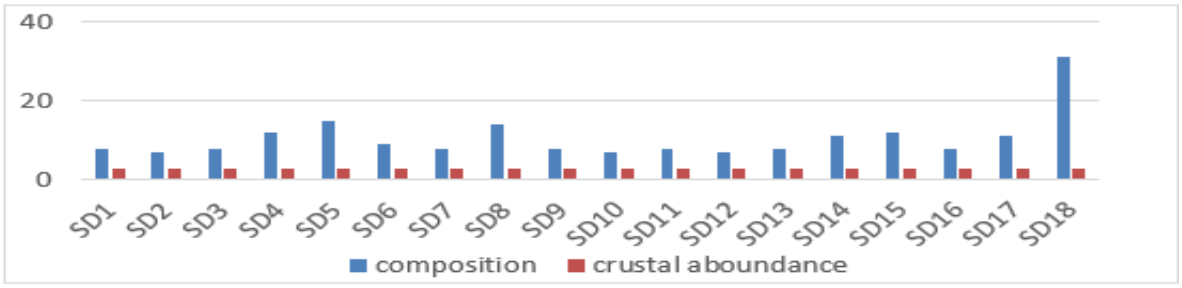

Figure 12: Bar chart comparing tantalum (Ta) concentrations in stream sediments with crustal abundance values

Tin (Sn): The concentration of **Sn**, as shown in the geochemical map, is higher within the pegmatite region of the Sisimbaki axis and eastern part of Arum Kadau.

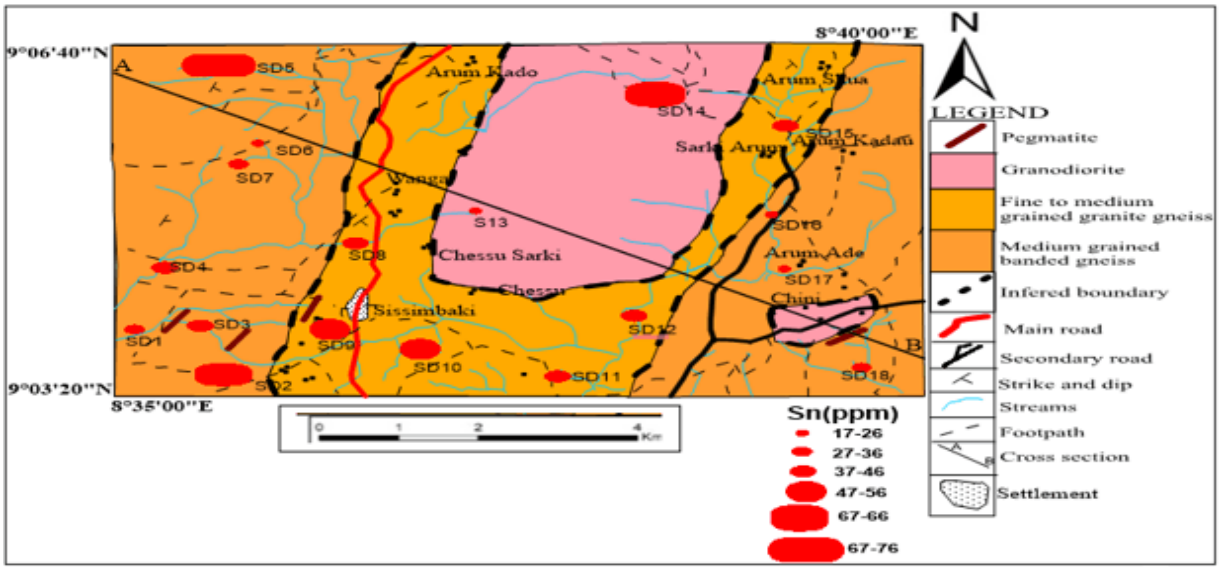

Figure 13: Spatial distribution map of tin (Sn) concentrations in stream sediments overlain on the geological map of Arum and environs

Figure 14: Bar chart comparing tin (Sn) concentrations in stream sediments with crustal abundance values

Uranium (U): Uranium concentration in the Arum environs, as shown in the geochemical map, is at the minimal. Though it is notably higher in southwestern part of Arum Chini

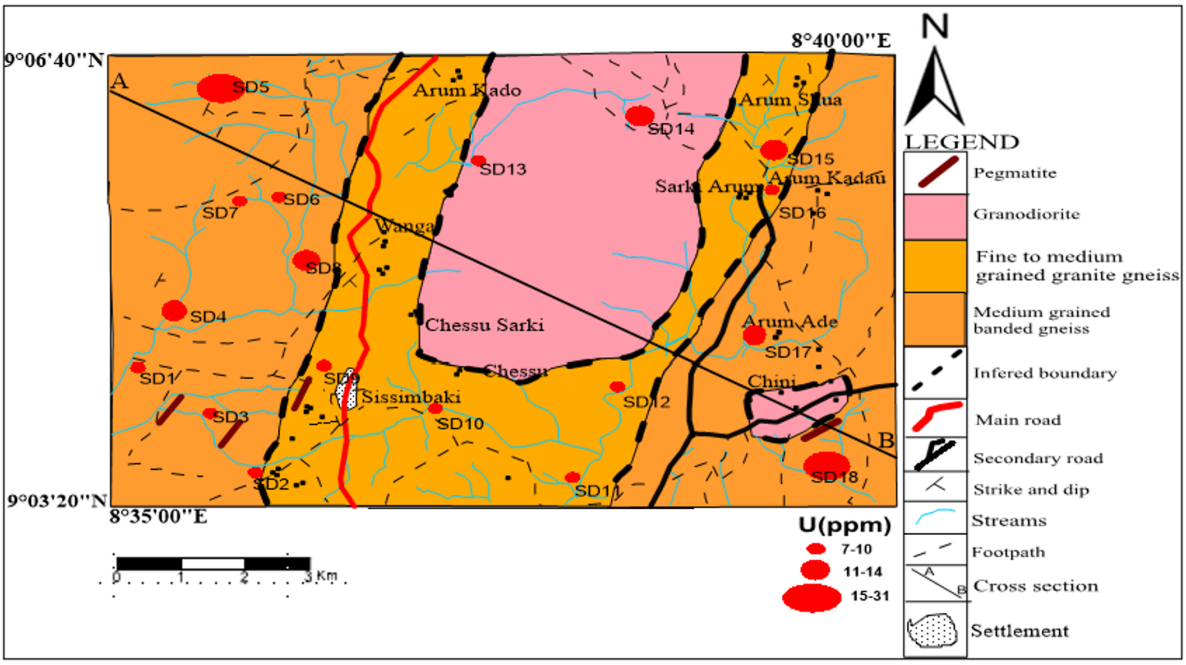

Figure 15: Spatial distribution map of uranium (U) concentrations in stream sediments overlain on the geological map of Arum and environs

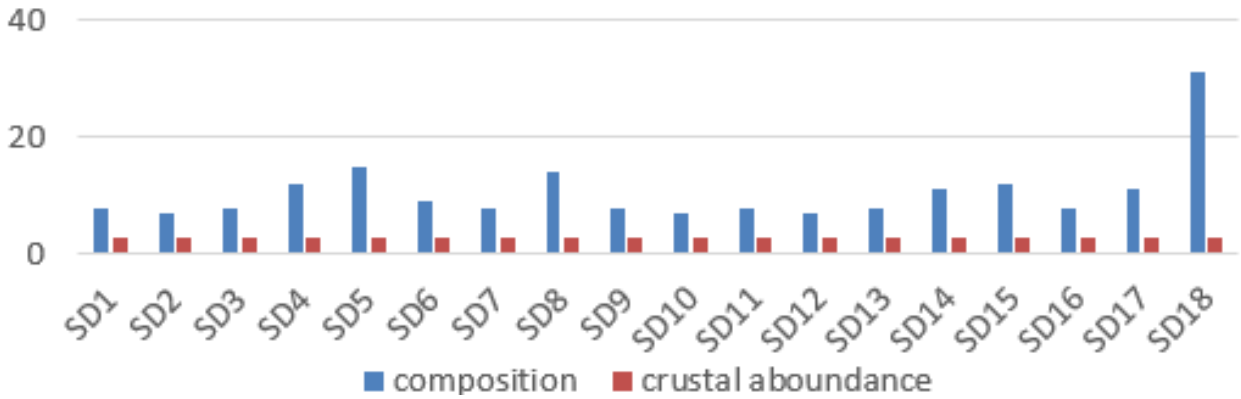

Figure 16: Bar chart comparing uranium (U) concentrations in stream sediments with crustal abundance values

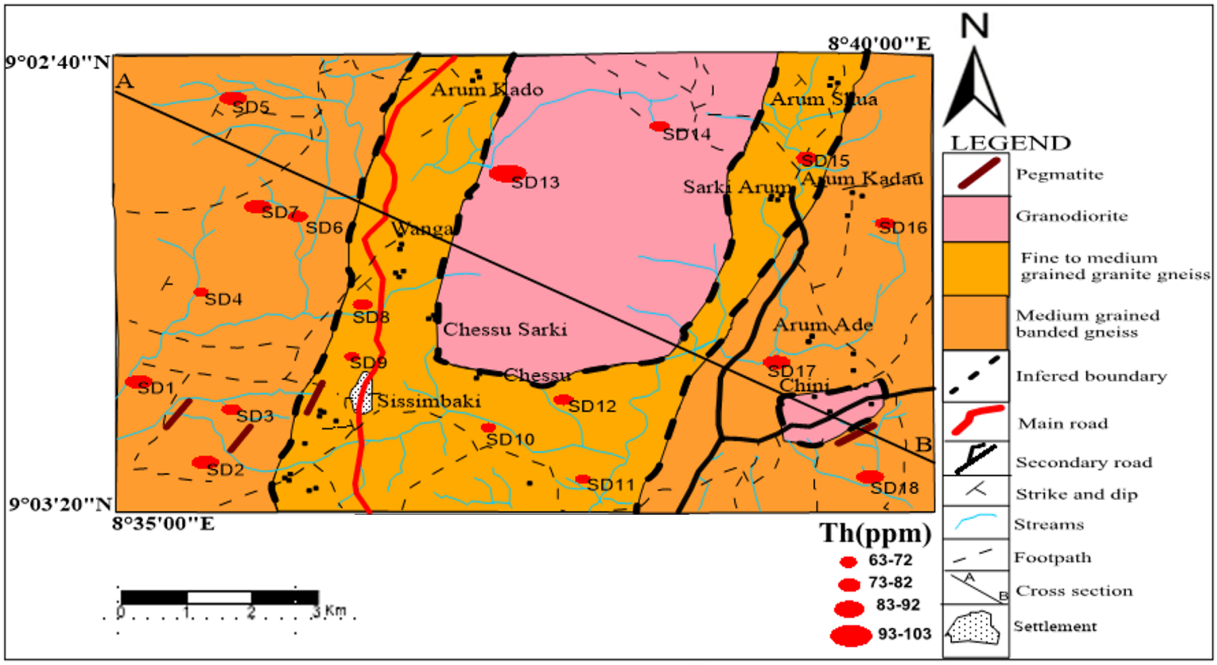

Figure 17: Spatial distribution map of thorium (Th) concentrations in stream sediments overlain on the geological map of Arum and environs

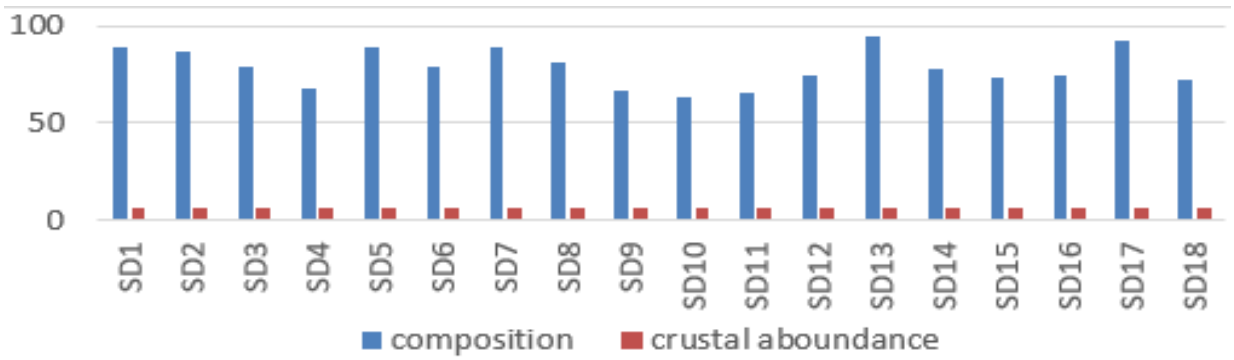

Figure 18: Bar chart comparing thorium (Th) concentrations in stream sediments with crustal abundance values

Figure 13 of tin (Sn) geochemical map shows elevated concentration of tin (Sn) in Arum, with much higher concentration around locations 2, 5 and 14 (Fig. 2), due to proximity to pegmatite and granodiorite. Analytical result shows that all samples collected within the coverage of granodiorite and pegmatite indicates higher values (5 – 81 and 9–19 ppm) while medium-grained banded gneiss and medium-grained granite gneiss with lower concentration, which could be the result of leaching, dissolution and transported from pegmatite bodies and/or granodiorite from within the study area.

Anudu *et al.* [27], worked on the structural and aeromagnetic data in part of North Central, which covered Arikya, Wamba and their environs, stated that the structural trends are responsible for the alluvial tin deposit and indicates that most streams are structurally controlled. These show that the structural patterns are responsible for some of the mineralization. Fig. 10 of the niobium (Nb) concentration plot shows a wide range of the element distribution across Arum, indicating anomalous tin (Sn) enrichment above the background values, with slight variation around medium-grain banded gneiss, probably due to lower concentration of Nb or could be due un-even weathering processes and structural migration channels. This enrichment and secondary mineralization process are prevalent in Arum and its adjoining areas.

Conclusion

This mineralogical has revealed three lithological units namely; the medium-grain banded gneiss MGBG, medium-grain granite gneiss MGGG and granodiorite G which are intruded by pegmatite. Also, geochemical similarly indicates the occurrence of granite, granodiorite and diorite, confirming the environment as being granitic and felsic in composition proving the igneous origin of the Arum rocks. It was also deduced from the geochemistry of the rocks that the rocks are

majorly calc-alkaline using. Trace elemental composition shows higher concentrations of Sn, Ta and Nb in pegmatite and granodiorite, while Th and U have the least concentration in all the rock types. Also, the soil geochemistry revealed a supergenetic enrichment in Nb, Ta, Sn, U and Th through weathering, transportation and their subsequent deposition from the surrounding rocks of Arum.

Conflict of interest/funding: The authors declare that, there is no competing interest and no funding was received for this work.

Acknowledgements: This paper is an excerpt from the lead-author's M.Sc research work which was also presented at the 2023 Nigeria Mining and Geosciences Society (NMGS) conference. Therefore, authors appreciate all the scholars who made useful contributions to the manuscript.

References

[1] Okunlola, O. A. (1998). Specialty metal potential of Nigeria. *Conference Proceedings of the First Mining in Nigeria* (pp. 67-90). A publication of the Federal Ministry of Solid Minerals Nigeria.

[2] Adekeye, J. I. D. & Akintola O. F., (2017). Geochemical features of rare-metal pegmatite in Nasarawa area Central Nigeria. *Journal of Mining and Geology* 43(1), 1– 21.

[3] Ogunleti, Y. S., Arikawe, E. A. & Okegye, J. I. K. (2014). Geochemical assessment of tin-tantalum mineralization in Precambrian pegmatite exposed at Angwan Rimi (Sheet 208 NE), North-central Nigeria. *Pacific Journal of Science and Technology*, 15(1), 415–425.

[4] Okunlola, O. A. (2005). Metallogeny of tantalum-niobium mineralization of *Precambrian pegmatites* of Nigeria. *Mineral Wealth*, 137, 38–50.

[5] Kuster, D. (1990): Rare-metal pegmatites of Wamba, central Nigeria – their Formation in relation to late Pan-Africa granites. *Mineral Deposita*, 25, 25–33. DOI: 10.1007/BF03326380

[6] Daspan, R. I., Yakubu, J. A. & Lar, U. A. (2007). Geochemical characteristics of gabbroic intrusive bodies in the Sha-Kaleri Younger Granite Complex, Central Nigeria. *Continental Journal of Earth Sciences*, 2, 7–13.

[7] Guagliardi, I., Apollaro, C., Scarciglia, F. & De Rosa, R. (2013a). Influence of particle size on geochemical distribution of stream sediments in the Lese River catchment, southern Italy. *Biotechnologie, Agronomie, Société et Environnement*, 17(1), 43–55.

[8] Guagliardi, I., Buttafuoco, G., Apollaro, C., Bloise, A., De Rosa, R. & Cicchella, D. (2013b). Using gamma-ray spectrometry and geostatistics for assessing geochemical behaviour of radioactive elements in the Lese catchment (southern Italy). *International Journal of Environmental Research*, 7(3), 645–658.

[9] Guagliardi, I., Buttafuoco, G., Cicchella, D. & De Rosa, R. (2013c). A multivariate approach for anomaly separation of potentially toxic trace elements in urban and peri-urban soils: An application in a southern Italy area. *Journal of Soils and Sediments*, 13(1), 117–128. https://doi.org/10.1007/s11368-012-0583-0

[10] Cozza, V., Guagliardi, I., Rubino, M., Cozza, R., Martello, A., Picelli, M. & Zhupa, E. (2015). ESOPO: Ensors and social pollution measurements. *CEUR Workshop Proceedings*, 1478, 52–57.

[11] Grant, N.K. (1970): Geochronology of Precambrian Basement Rocks from Ibadan, southwestern Nigeria. *Earth and Planetary Science Letters* 10, 29-38.

[12] Ajibade. A. C, Woakes, M. & Rahaman M.A (1987): Proterozoic Crustal Development in the Pan-African Regime of Nigeria. In: C. A. Kogbe, *Geology of Nigeria* 2nd revised edition (pp. 57-69). Rock View Nigeria Limited, Jos.

[13] Dada, S. S., Birck, J. L., Lancelot, J. R. & Rahaman, M. A. (1993): Archean migmatite-gnesis complex of North Central Nigeria: its geochemistry, Petrogenesis and crustal evolution. In *16th International Colloquium on African Geology* (1, 97–102). Mbabane, Swaziland, Extended Abstracts.

[14] Dada, S. S. (1998). Crust-forming ages and Proterozoic crustal evolution in Nigeria: A reappraisal of current interpretations. *Precambrian Research*, 87, 65-74.

[15] Dada, S.S. (2008). Proterozoic evolution of the Nigeria-Borborema Province. In: R. J. Pankhurst, R. A. Trouw, B. B. Brito Neves and M. J. De Wit, *West Gondwana: Pre-Cenozoic Correlations across the South Atlantic Region* (pp. 121-136). Geological Society of London Special Publication, London.

[16] Burke, K. C. & Dewey, J. F., (1972). Orogeny in Africa. *In: African Geology*, T.F.J. Dessauvagie and A. J. Whiteman (pp. 583-608). Ibadan: University of Ibadan Press.

[17] Leblanc, M., (1981). The late Proterozoic ophiolites of BouAzzer (Morocco): Evidence for Pan-African plate tectonics. In: Kroner, A., *Precambrian Plate Tectonics* (pp. 435 -451). Elsevier Amsterdam.

[18] Black, R., Caby R. & Moussine-Pouchkine, A. (1979). Evidence for late Precambrian plate tectonics in West Africa. *Nature*, 278, 223–226.

[19] Caby, R., Betrand, J. M. I. & Black, R., (1981). Pan-African Ocean closure and continental collision in the Hoggar-Iforas segment, Central Sahara. In: A. Kronaer edition, *Precambrian Plate Tectonics* (pp. 407-434). Elsavier, Amsterdam.

[20] Garba, I. (2002). Late Pan-African tectonics and origin of gold mineralization and rare metals pegmatites in the Kushaku Schist Belt, North Western Nigeria. *Journal of Mineralogy and Geology*, 3(1), 1-12.

[21] Adekeye, J. I. D. & Akintola O. F. (2017). Geochemical features of rare-metal pegmatite in Nasarawa area Central Nigeria. *Journal of Mining and Geology*, 43(1), 1– 21.

[22] Jimoh, R. O. (2018). Geochemical characterisation of tourmaline and beryl from selected gem-bearing pegmatites in southwestern Nigeria (Doctoral thesis, University of Ibadan).

[23] Ilaria Guagliardi, Nicola Ricca & Domenico Cicchella (2016). Geochemical pathway of elements in Cosenza and Rende area (Calabria, southern Italy). *Geol. It.*, 38, 55-58. (DOI: 10.3301/ROL.2016.16) © Società Geologica Italiana, Roma 2016

[24] Cox, K. G., Bell, J. D. & Pankhurst, R. J. (1979). *The Interpretation of Igneous Rocks*. London: Allen & Unwin.

[25] Irvine, T. N. & Baragar, W. R. A. (1971). A guide to the chemical classification of the common volcanic rocks. *Canadian J. of Earth Sci.*, 8(5), 523–548. https://doi.org/10.1139/e71-055

[26] Jatau, B.S Oloniniyi L. T., Tanko Y.I and Hanly Bingari(2012): Preliminary stream sediments analysis for gold prospecting at Ragga and environs part of Kurra sheet 189 SW North-Central Nigeria. Book of proceedings of Akure 2013 AGM/Conference @ Nigeria Society of Mining Engineering. Pp 62-70.

[27] Anudu, G. K., Obrike, S. E., Iyakwari, S. & Ikpokonte, A. E. (2012). Preliminary structural study of LANDSAT imagery over Wamba and environs, Nasarawa State, Northcentral Nigeria. *Res. Journal of Applied Sci.*, 7(1), 1–9. https://doi.org/10.36478/rjasci.2012.1.9

Citing this Article

Usman, A. S., Segun, A. B., Kaura, A. M., Mukaila, A. S., Andarawus, Y., Sanusi, I. M., Aliyu, S., Agho, L. O. & Bamidele, T. E. (2026). Geochemical characterization and mineralization potential of basement rocks in Arum, North-Central Nigeria. *Lafia Journal of Scientific and Industrial Research*, *4*(1), 176–188. https://doi.org/10.62050/ljsir2026.v4n1.727